Two-photon photovoltaic effect in gallium arsenide

Jichi Ma,[1] Jeff Chiles,[1] Yagya D. Sharma,[2] Sanjay Krishna,[2] and Sasan Fathpour[1,3,*]

[1]*CREOL, The College of Optics and Photonics, University of Central Florida, Orlando, Florida 32816, USA*

[2]*Center for High Technology Material, University of New Mexico, Albuquerque, New Mexico 87106, USA*

[3]*Department of Electrical Engineering and Computer Science, University of Central Florida, Orlando, Florida 32816, USA*

**Corresponding author: fathpour@creol.ucf.edu*

Received June 24, 2014; revised August 4, 2014; accepted August 5, 2014;
posted August 7, 2014 (Doc. ID 214669); published September 4, 2014

The two-photon photovoltaic effect is demonstrated in gallium arsenide at 976 and 1550 nm wavelengths. A waveguide-photodiode biased in its fourth quadrant harvests electrical power from the optical energy lost to two-photon absorption. The experimental results are in good agreement with simulations based on nonlinear wave propagation in waveguides and the drift-diffusion model of carrier transport in semiconductors. Power efficiency of up to 8% is theoretically predicted in optimized devices. © 2014 Optical Society of America

OCIS codes: (250.4390) Nonlinear optics, integrated optics; (230.0250) Optoelectronics; (040.5350) Photovoltaic; (130.4310) Nonlinear.

http://dx.doi.org/10.1364/OL.39.005297

The two-photon photovoltaic (TPPV) effect is harvesting the energy of the photons lost to two-photon absorption (TPA) [1]. The effect is a nonlinear equivalent of the conventional (single-photon) photovoltaic effect widely used in solar cells. One possible application of the TPPV effect is self-powered electronic–photonic integrated circuits, in which the harvested energy can be used to drive electrical circuits on the same chip [2]. A good example is self-powered in-line monitors (or optically powered remote sensors) in fiber-optic networks [3]. Another potential application of the TPPV effect is remote power delivery to physical sensors installed in critical environments where electrical sparks are dangerous and copper cables must be avoided [2].

The TPPV effect was first demonstrated in silicon [1]. Although the main purpose was to eliminate the nonlinear losses in silicon waveguides [TPA and free-carrier absorption (FCA)] by decreasing the carrier lifetime while, simultaneously, net electrical energy was harvested with reasonable power efficiency. Energy harvesting (or negative electrical power dissipation) based on the TPPV effect in silicon has been specifically investigated in Raman amplifiers [4], parametric wavelength converters [5], and optical modulators [6].

TPA has been long observed experimentally in gallium arsenide (GaAs) and the corresponding coefficient, β, reported in GaAs at 1.3 μm is 42.5 cm/GW, which is much higher than silicon's (3.3 cm/GW) [7]. At the telecommunication wavelength of 1.55 μm, β is reported to be around 15 cm/GW in GaAs [8,9] compared with 0.7 cm/GW in silicon. Thus, the TPPV effect is expected to be stronger in GaAs. In this Letter, the TPPV effect is demonstrated in GaAs for the first time.

In principle, every two photons lost to TPA generate one electron–hole pair in the semiconductor material and these photogenerated carriers are available for photovoltaic conversion into electrical power. Figure 1(a) shows the TPA process at the two particular wavelengths studied here, i.e., 976 and 1550 nm. Figure 1(b) shows a simplified schematic on how nonlinear absorption along the waveguide (due to TPA at high optical intensities) is different than linear absorption at low intensities. FCA is ignored in this simplified diagram. Figure 2 illustrates how TPPV can be realized in a single-mode GaAs/AlGaAs waveguide using a p-i-n junction diode. The employed device resembles a standard edge-emitting laser but without any active (quantum well) region.

A theoretical model is developed to describe the TPPV effect in the GaAs/AlGaAs waveguide with vertical p-i-n heterojunction diodes, as shown in Fig. 2. Although a o1-D model is enough for simulation of conventional solar cells, a 2-D approach that considers the optical intensity distribution of the guided mode is applied here. The numerical model is developed in COMSOL's Multiphysics module. The model solves the drift-diffusion equations of carrier transport in semiconductors in terms

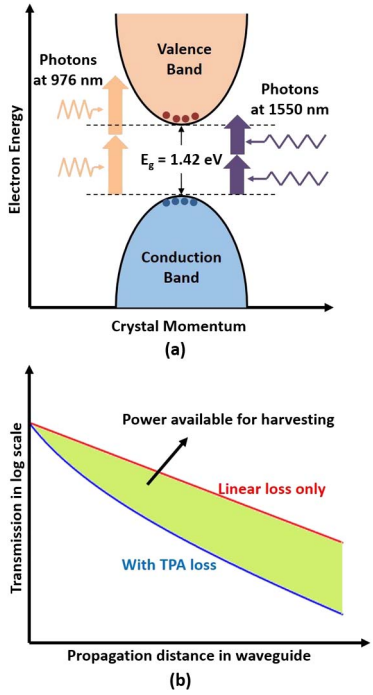

Fig. 1. (a) TPA in GaAs at studied wavelengths of 976 and 1550 nm and (b) waveguide loss with and without TPA. The carriers generated in GaAs by TPA are in principle available for photovoltaic conversion (FCA has been ignored in this simplified diagram).

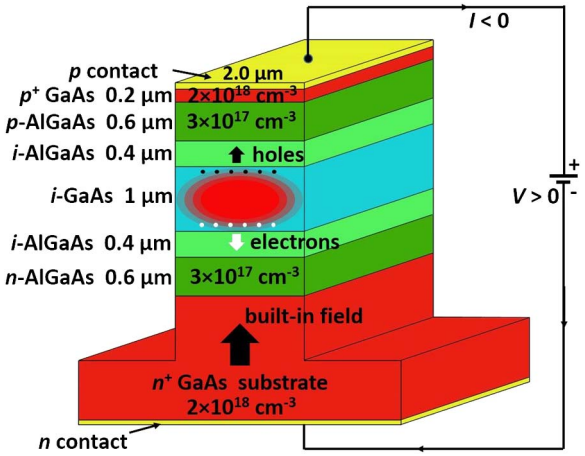

Fig. 2. Schematic of a GaAs/AlGaAs waveguide diode for photovoltaic power conversion using the process in Fig. 1(a).

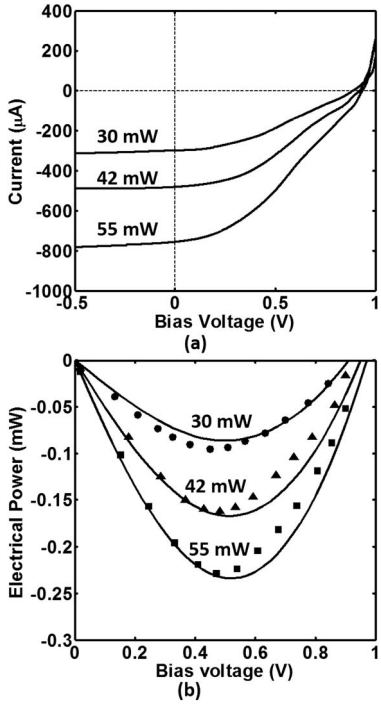

Fig. 3. (a) I–V characteristics of the diodes at wavelength of 976 nm for three different coupled input powers and (b) the corresponding P–V characteristics of the diodes from numerical simulation (solid line) and experiment (circles, triangles, and squares).

of the quasi-Fermi potentials along with Poisson's equation [10].

The Shockley–Read–Hall recombination is taken into account in this model assuming the trap energy level is located at the middle of the bandgap. The electron and hole bulk recombination lifetimes, τ_n and τ_p, in bulk GaAs are of the order of 10^{-8} s, about 2 orders of magnitude smaller than those in bulk silicon. In GaAs/AlGaAs waveguides, the effective free-carrier lifetime τ_{eff} can be even smaller when the surface recombination at the waveguide sidewalls dominates over the bulk recombination. τ_{eff} of 250 ps is reported for a 2.4 μm × 0.8 μm GaAs/$Al_{0.8}Ga_{0.2}$As ridge waveguide [11]. In this work, τ_{eff} is assumed to be 100 ps, as good agreement between numerical simulation and experimental data is achieved with this value [Figs. 3(b) and 5(b))]. This low value suggests that the lifetime is dominated by surface rather than bulk recombination. This value is reasonable considering the sidewall roughness induced by the dry etching process, which may have increased the surface recombination. Surface recombination reduces the power efficiency of the TPPV effect as the electrons and holes recombine before they are collected at the contacts. Higher τ_{eff} can be achieved by optimizing the dry etching recipe and smoothening the sidewalls of the waveguide. Table 1 summaries the other parameters and material properties used in the simulation.

From the current density, J, calculated by COMSOL, the total current is calculated by integrating J over the waveguide length, L. Finally, the ohmic loss of the electrodes and the contacts is included as a series resistance, R_s, in the circuit. The ohmic loss will reduce the harvested electrical power and might possibly lower the short-circuit current if R_s is excessively high.

It should be noted that the waveguide in Fig. 2 is multimode at both wavelengths studied in this work. As the carrier photogeneration rate is proportional to the square of the optical intensity, the intensity distribution across the cross section of the waveguide is not expected to be important as far as the mode and the coupled input optical power are well confined in the GaAs core layer. It was confirmed by simulation that, for the same coupled input power, the change in the collected current density is negligible when the intensity distribution of fundamental and higher order modes are compared. This can also be explained mathematically by a simplified 1-D model for slab waveguides, assuming the electric field in the waveguide core follows a cosine function and drops to zero at the core–cladding interface.

Table 1. Material Properties Used in This Study

Parameters	Unit	GaAs	$Al_{0.15}Ga_{0.85}As$
Relative permittivity ε_r 976 nm	—	12.42	11.88
1550 nm	—	11.41	11.27
Intrinsic carrier density n_i	cm^{-3}	2.2×10^6	6.6×10^4
Electron mobility μ_n	$cm^2/(Vs)$	8500	4925
Hole mobility μ_p	$cm^2/(Vs)$	400	241
Effective mass of electron m_e	m_0	0.067	0.076
Effective mass of hole m_h	m_0	0.48	0.548
Energy bandgap E_g	eV	1.42	1.611
Electron affinity X	eV	4.06	3.905

The heterostructure in Fig. 2 was grown by molecular beam epitaxy and several devices with identical widths of 2.0 μm but varying etch depths were fabricated using standard optical lithography, lift-off, and dry etching processes. The length of all the waveguides reported here is 4.5 mm.

For characterization of the devices, optical energy is coupled into the intrinsic GaAs layer (waveguide core) through a lensed fiber. The coupling loss is estimated to be around 6 dB. Two wavelengths, one closer to GaAs's bandgap (from a high-power 976 nm diode laser) and 1550 nm (from an erbium-doped fiber amplifier) were studied. The choice of these wavelengths is merely based on the high-power sources available to us.

The linear propagation loss, α, of the waveguide is measured by the cut-back method and is estimated to be 7 dB/cm at 976 nm and around 18 dB/cm at 1550 nm. The high linear loss at 1550 nm can be explained by the mode leakage into the n^+-GaAs substrate as the AlGaAs bottom cladding layer is only 1 μm thick, as confirmed by the imaginary part of simulated effective index. To reduce the mode leakage and increase the power efficiency of the device at this longer wavelength (1550 nm), the bottom cladding layer has to be thicker than 2 μm. The current–voltage (I–V) characteristics of the fabricated waveguide diodes were measured with a curve tracer at various coupled pump powers and wavelengths.

Figure 3(a) shows the measured I–V characteristics at 976 nm at three different coupled input powers. The etch depth of the ridge waveguide is 4.2 μm (all the way down to the n^+-GaAs substrate). The TPPV effect is clearly observed when the device is biased in the fourth quadrant of its I–V characteristics, i.e., the carriers generated by TPA are swept out by the built-in field of the p-i-n junction and collected at the electrodes. The measured current is a combination of the photocurrent (from TPA), the minority carrier diffusion current, and the recombination current (including both bulk and surface recombination).

The power–voltage (P–V) characteristics of the diode at three different coupled input powers are shown in Fig. 3(b). Evidently, 230 μW of electrical power can be scavenged from this device. The solid lines show agreeable simulation results based on the model described before. R_s and β are treated as fitting parameters in the simulation and are estimated to be around 700 Ω and 40 cm/GW, respectively. The β value obtained here is comparable to those reported in [7,9].

It should be mentioned that the device has also been tested before annealing. At pump power of 55 mW, the generated electrical power is only half of that harvested from an annealed device. This indicates that annealing alleviates the ohmic loss remarkably and is crucial in fabrication of the photovoltaic devices. Up to 9% power efficiency, excluding the coupling loss, is theoretically predicted in long (several centimeters), low-loss GaAs waveguides [2]. The rather low wall-plug efficiency observed here is attributed to the high series resistance at the contacts, as well as fabrication imperfections, which result in high linear propagation loss and strong surface recombination at the sidewalls of the waveguide.

Figure 4(a) shows the I–V characteristics of a similar device at 976 nm, but with a shorter etch depth of 1.0 μm

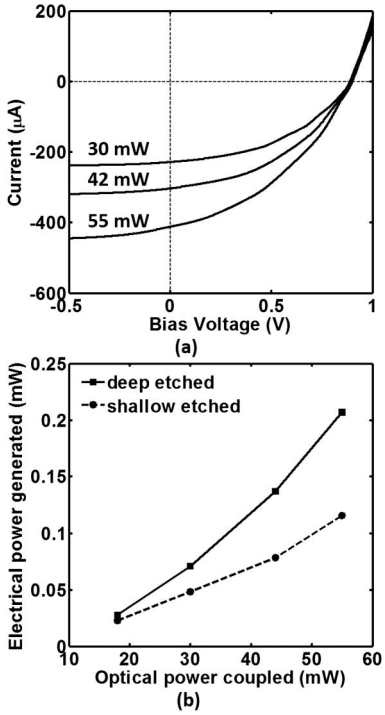

Fig. 4. (a) Measured I–V characteristics of the shallow-etched devices at wavelength of 976 nm for three different coupled input powers. (b) Measured electrical power generated in a 1 kΩ load resistance for both etch depths.

(down to the center of the AlGaAs cladding layer). The shallow-etched device has two advantages. First, since the GaAs core layer is not fully etched, the scattering loss of the optical mode is less and the surface recombination is weakened; second, the selectivity of the applied dry etching process between GaAs and gold is around 20:1. Therefore, the top contact gold layer is around 150 μm thicker than that of the deep-etched device due to less etching time in the process, which decreases R_s by about 200 Ω. However, the generated photocurrent and the harvested electrical power are less than those in the deep-etched device because of the existence of a huge slab mode, which results in low optical intensity in the waveguide core, i.e., the photons generated in the slab cannot be efficiently collected by the diode. Figure 4(b) presents the measured electrical power harvested and delivered to a load resistance of 1 kΩ, for the two studied etch depths.

Next, TPPV in GaAs was studied at the telecommunication wavelength of 1550 nm. The etch depth of the ridge waveguide is 4.2 μm in this case. The I–V and P–V characteristics measured at three different coupled input powers are shown in Figs. 5(a) and 5(b), respectively. Once again, good agreement between the numerical and experimental results is observed. β is estimated to be 17 cm/GW at this wavelength, in accordance with the value reported in [8,9], and is still much higher than that in silicon (0.7 cm/GW at 1550 nm). The maximum scavenged electrical power is ~220 μW.

Finally, to predict the ultimate performance limit of GaAs TPPV power converters, devices with more idealistic, but reasonable, conditions were simulated. Negligible ohmic loss of the contacts, as well as low linear propagation loss of 1 dB/cm are assumed in this

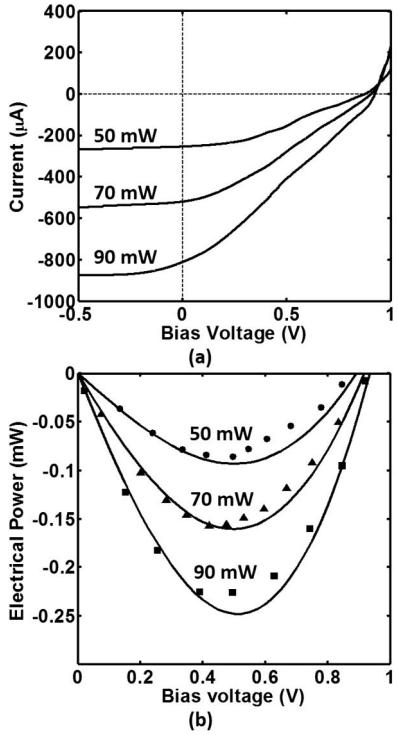

Fig. 5. (a) I–V characteristics of the diodes at wavelength of 1550 nm for three different coupled input powers and (b) the corresponding P–V characteristics of the diodes from numerical simulation (solid line) and experiment (circles, triangles, and squares).

simulation. Such low α is achievable in micrometer-sized waveguides if the bottom cladding layer is designed to be thicker and the fabrication processes, especially the dry etching recipe, are optimized.

Figure 6 presents the simulated maximum possible generated electrical power versus input power for three different waveguide lengths at 1550 nm. 12 mW of electrical power can be harvested at input power of 150 mW in a 5-cm-long device, i.e., a power efficiency of 8%. At higher input power, a slight increase in the slope is clearly visible in all three lines [as well as in Fig. 4(b)]. This does not occur in silicon (Fig. 5 of Ref. [1]) due to the high FCA loss in silicon waveguides. Further increasing the length of the present GaAs waveguide can only slightly improve the power efficiency as the optical intensity is not high enough after the light propagates a certain distance along the waveguide and gets absorbed gradually.

In conclusion, the TPPV effect is experimentally demonstrated in GaAs for the first time at wavelengths of 976 and 1550 nm. Good agreement between the simulation and experimental results is observed. The TPPV effect is more efficient at 976 nm due to larger β. A maximum

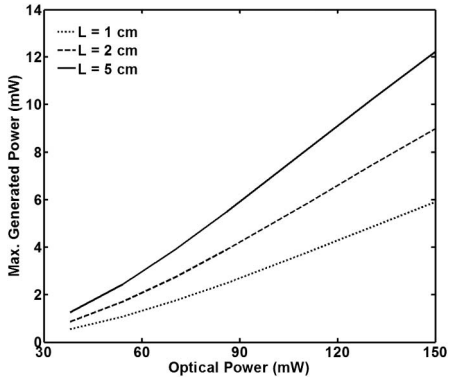

Fig. 6. Theoretical limit of electrical power generation versus coupled optical power for three different device lengths of 1, 2, and 5 cm at 1550 nm wavelength.

electrical power of 230 μW is generated with 90 mW coupled input power at 1550 nm. Higher power efficiency at 1550 nm can be achieved by optimizing the waveguide design, particularly by increasing the thickness of the intrinsic bottom cladding layer. Power efficiency up to 8% is theoretically predicted in a 5-cm-long device at input power of 150 mW, which is higher than those achievable in silicon.

The work is supported by the U.S. National Science Foundation under award ECCS-1128208.

References

1. S. Fathpour, K. Tsia, and B. Jalali, IEEE J. Quantum Electron. **43**, 1211 (2007).
2. S. Fathpour, K. Tsia, and B. Jalali, in *Silicon Photonics for Telecommunications and Biomedicine*, S. Fathpour and B. Jalali, eds. (CRC, 2012), pp. 363–381.
3. B. Jalali, S. Fathpour, and K. Tsia, Opt. Photon. News **20**(6), 18 (2009).
4. S. Fathpour, K. Tsia, and B. Jalali, Appl. Phys. Lett. **89**, 061109 (2006).
5. K. Tsia, S. Fathpour, and B. Jalali, Opt. Express **14**, 12327 (2006).
6. S. Fathpour and B. Jalali, Opt. Express **14**, 10795 (2006).
7. H. F. Tiedje, H. K. Haugen, and J. S. Preston, Opt. Commun. **274**, 187 (2007).
8. A. Villeneuve, C. C. Yang, G. I. Stegeman, C. N. Ironside, G. Scelsi, and R. M. Osgood, IEEE J. Quantum Electron. **30**, 1172 (1993).
9. S. Krishnamurthy, Z. G. Yu, L. P. Gonzalez, and S. Guha, J. Appl. Phys. **109**, 033102 (2011).
10. M. S. Lundstrom and R. J. Schuelke, IEEE Trans. Electron Devices **ED-30**, 1151 (1983).
11. P. Apiratikul, "Semiconductor waveguides for nonlinear optical signal processing," Ph.D. dissertation (University of Maryland, 2009).